JOURNAL OF MATERIALS SCIENCE 14 (1979) 1389–1397

Tempering of a beta quenched Zr–1.9 wt % Cr alloy

Part 1 *Martensite structure*

P. MUKHOPADHYAY, V. RAMAN, S. BANERJEE, R. KRISHNAN
Metallurgy Division, Bhabha Atomic Research Centre, Bombay-400085, India

The morphology and the substructure characterizing the martensite produced on beta quenching a Zr–1.9 wt % Cr alloy have been examined by optical and transmission electron microscopy. The structural changes that occur in the martensite structure on tempering at various temperatures in the α + $ZrCr_2$ phase field have also been investigated.

1. Introduction

The binary zirconium–chromium system is a beta eutectoid system where the intermetallic phase formed in the eutectoid reaction [1] β-Zr(Cr) → α-Zr(Cr) + $ZrCr_2$ has the stoichiometry $ZrCr_2$ and is a topologically close-packed Laves phase [2]. It appears that the eutectoid composition depends quite markedly on the oxygen content. Oxygen strongly stabilizes the alpha-phase while chromium stabilizes the beta phase only mildly [3]. While Domagala *et al.* [1] have found that the eutectoid point occurs at 1.0 wt % chromium in an alloy containing about 100 ppm oxygen, Hayes *et al.* [4] have observed that when the oxygen concentration is about 1000 ppm, the eutectoid composition corresponds to about 1.8 wt % chromium. More recently, Rumball and Elder [3] have also found that oxygen increases the chromium concentration of the eutectoid from between 0.7 and 0.95 wt % for an oxygen-free alloy to 1.25 wt % for an alloy containing 2400 ppm oxygen. The zirconium-rich end of the binary zirconium–chromium phase diagram [1] is shown in Fig. 1. It can be seen that the solubility of chromium is very small in alpha zirconium and considerably larger in beta zirconium. Quenching dilute alloys of appropriate compositions from the beta field at rapid rates should bring about the martensitic beta to alpha prime transformation and in view of the extremely restricted solubility of chromium in the alpha phase, the martensite would be supersaturated. If the cooling rate is not fast enough, it is possible that a fraction of the chromium atoms would be thrown out of the zirconium lattice so that precipitation would occur during the quenching process. Progressive additions of chromium would be expected to lower the M_s temperature and at an appropriately high concentration, where this temperature is reduced below the ambient, rapid beta quenching would lead to the retention of the beta phase in a metastable form at room temperature. In view of the experience gained with reference to other zirconium and titanium base alloys (with alloying additions that tend to stabilize the beta phase), the formation of the omega phase would also be

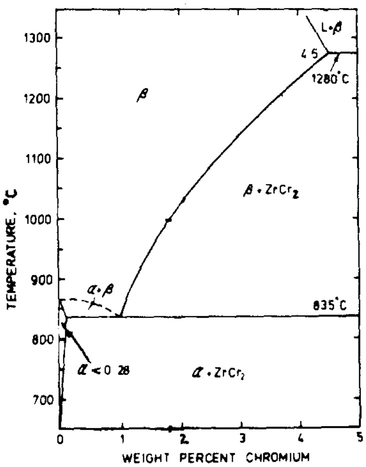

Figure 1 The zirconium-rich end of the binary zirconium–chromium phase diagram. (After [1]).

expected once the amount of chromium is sufficient for beta retention [5]. Subsequent ageing of these dilute beta quenched alloys (martensitic or otherwise) at temperatures lower than the eutectoid temperature would lead to the emergence of $ZrCr_2$ precipitates.

It has been reported [6] that zirconium–chromium alloys containing up to about 1.8 wt% chromium, on rapid beta quenching, are fully transformed into martensite. Further chromium enrichment leads to a progressive reduction in the amount of martensite in the quenched product and a corresponding rise in the volume fraction of the omega phase; at a chromium content of 2.5 wt%, the beta quenched alloy consists entirely of the omega phase. One peculiar characteristic of this system appears to be that unlike in most other zirconium- and titanium-base alloys where this phase forms, the beta to omega transformation can be achieved here without the retention of the beta phase [3, 6].

The work reported in this paper was undertaken with a view to studying the morphology and the substructure of the martensite in a Zr–1.9 wt% Cr alloy and examining the stability of the martensite structure on tempering.

2. Experimental details

The alloy was received in the form of a 1 mm thick strip which was cold-rolled down to 0.3 mm thickness. This rolled alloy was cut into appropriate pieces for optical and electron microscopy and X-ray diffraction. These pieces were wrapped in tantalum foil and encapsulated in silica capsules in a protective atmosphere of helium (175 mm pressure). Beta solutionizing was carried out at 1200° C for 30 min. This was followed by rapid quenching. Tempering was carried out at three temperatures: 350, 550 and 700° C for different periods of time. Chemical analysis of the post-heat-treated alloy showed that it contained 1.89 wt% chromium, 950 ppm oxygen and 60 ppm nitrogen.

Chemical thinning/etching was carried out using a solution of 5 parts hydrofluoric acid, 45 parts nitric acid and 50 parts water. The electropolishing solution for thin foil preparation contained 30 parts perchloric acid, 175 parts *n*-butanol and 300 parts methanol. The temperature of this solution was maintained below −50° C during polishing. The "window" technique was employed. Polishing voltages were in the range 20 to 30 V and the cathode was of stainless steel.

3. Results and discussion

3.1. Beta quenched structure

Optical microscopy of the beta quenched alloy revealed that most of the beta grains had undergone the martensitic transformation. However, a small number of grains appeared to have remained untransformed. The typical appearances of the transformed and the "untransformed" grains are shown in Fig. 2. It could be seen from Fig. 2b that some phase transformation had occurred in the vicinity of the boundaries separating the "untransformed" grains. This was a feature common to all such regions. The martensite structure in this alloy at the level of optical metallography examination, could be categorized as one having an acicular or plate morphology. This observation was based on the fact that the martensite units, in general, possessed a lenticular shape and that neighbouring

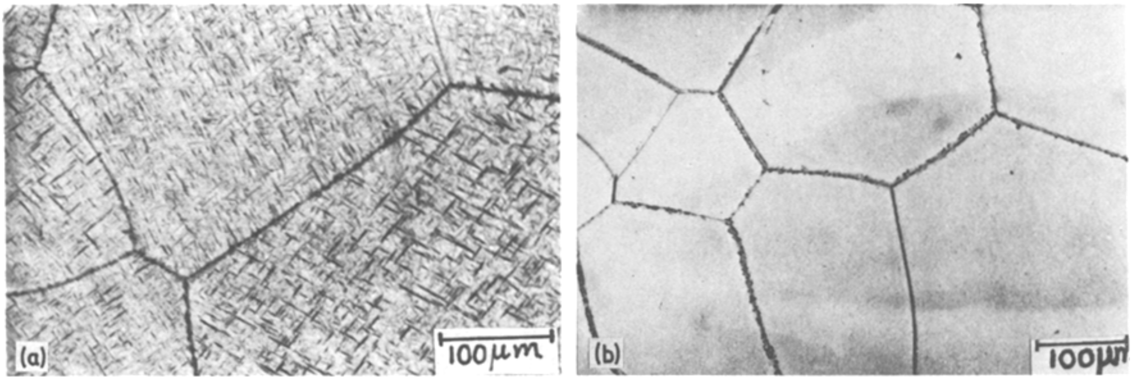

Figure 2 Typical appearance of (a) the martensitic and (b) the non-martensitic regions of the beta quenched alloy, as observed in the light microscope.

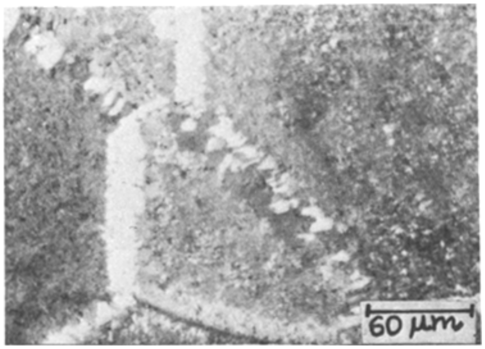

Figure 3 Polarized light micrograph from an apparently untransformed region in the beta quenched alloy showing the grain-boundary phase and the dispersion of a similar phase in the interior of the grains.

martensite crystals belonged to different orientation variants. Polarized light microscopy of the apparently untransformed grains revealed that these grains contained a dispersion of a phase which reacted to polarized light in a manner similar to the grain-boundary phase (Fig. 3). This suggested that the apparently untransformed grains were not really untransformed. Microhardness measurements across the grain boundaries showed that the grain-boundary phase was much harder than the grain interior.

X-ray diffraction was employed to identify the phases present in the beta quenched alloy. All the samples examined gave rise exclusively to alpha zirconium peaks implying that the volume fractions of the other phases was very small. However, it should be borne in mind that the strongest beta zirconium peak (i.e. $\{1\,1\,0\}$) is nearly coincident with the $\{0\,0\,0\,2\}$ alpha zirconium peak and that these peaks are difficult to resolve. Moreover, the $\{1\,0\,\bar{1}\,1\}$ and the $\{1\,1\,\bar{2}\,0\}$ peaks of the omega phase also occur nearly at these angles. It is pertinent to note that the relative intensity of the $\{0\,0\,0\,2\}_\alpha$ peak was found to be much larger than what would be expected if the grains were randomly oriented (Fig. 4). This enhancement in intensity might have corresponded to a superposition of peaks from different phases. On the other hand, it was also possible that the alloy had developed a moderate basal texture during the fabrication and heat-treatment schedule.

In transmission electron microscopy, the morphology of the martensite appeared to be a mixed one. In some regions the martensite units were observed to have formed along intersecting directions (Fig. 5a) while in some other locations a near parallel stacking could be noticed (Fig. 5b). Selected-area diffraction from adjacent martensite crystals, even from some regions of parallel stacking, showed that these crystals were often twin related (Fig. 6), the twin plane being of the $\{1\,0\,\bar{1}\,1\}$ type. This was in contrast to the observation made in pure zirconium [7] where the lath martensite colonies consist of parallel stacked crystals of near-identical orientations. The observation of twin related laths in a colony in the present case suggested that the two variants of the beta–alpha orientation relation operative in such pairs of laths were twin related. This was possible because some (four out of six, to be exact) $\{1\,0\,\bar{1}\,1\}$ planes are derived from the $\{1\,1\,0\}$ type mirror planes of the parent beta crystal [8].

The beta–alpha orientation relation associated with the martensitic transformation in this alloy could not be determined directly because the transformation was complete in the grains which showed the martensitic structure. However, the operation of the Burgers orientation relation [9], which is valid for the beta to alpha transformation in several zirconium and titanium base alloys, could be confirmed indirectly from diffraction patterns obtained from regions covering several

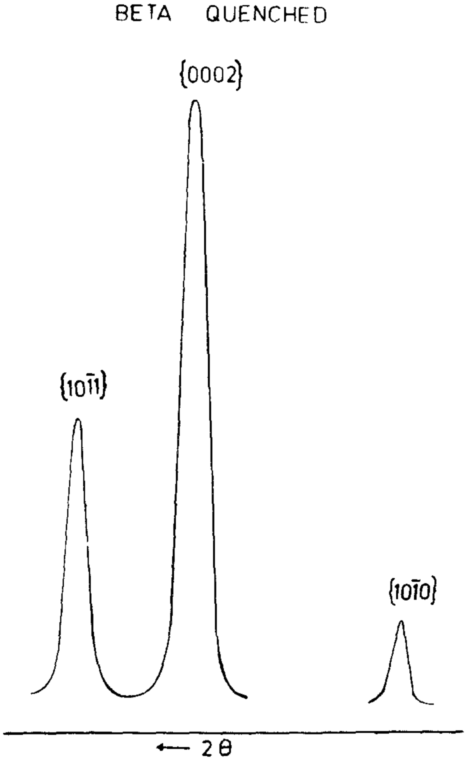

Figure 4 X-ray diffraction profile showing the enhanced intensity of the (0 0 0 2) reflection in the beta quenched alloy.

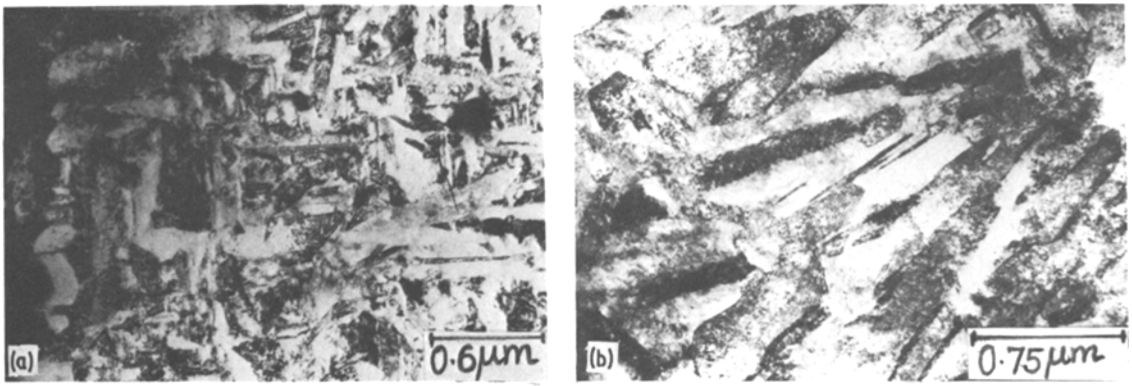

Figure 5 (a) Formation of martensite units along intersecting directions in the beta quenched alloy. (b) Near parallel stacking of martensite crystals in a colony in the beta quenched alloy.

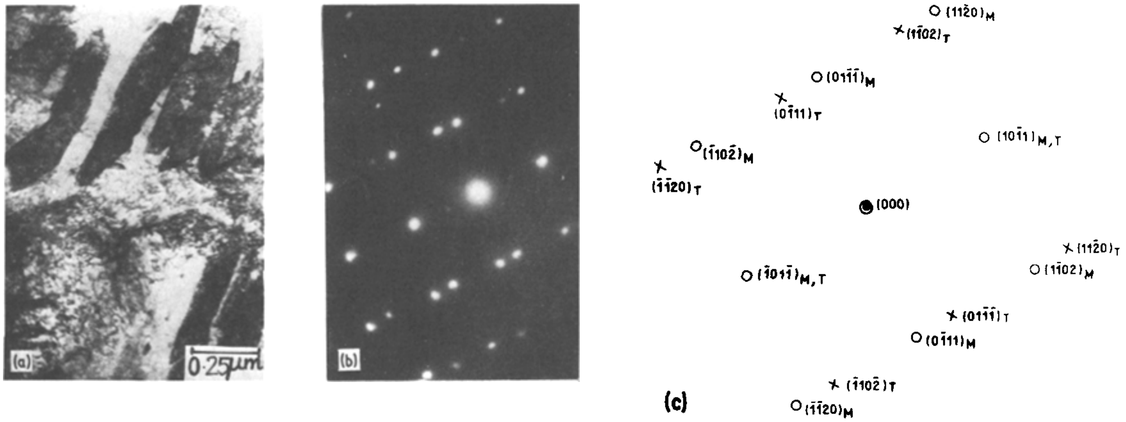

Figure 6 Zr–1.9 wt% Cr, beta quenched; illustrating twin-related laths. (a) Parallel stacking of laths, (b) selected-area diffraction pattern from the region shown in (a). Zone axis: $\langle 1 0 \bar{1} 1\rangle$ type. (c) Key to the diffraction pattern in (b). The subscripts M and T refer to the two twin-related orientations.

variants of martensite crystals. An example is given in Fig. 7a in which the reciprocal lattice sections of three different alpha crystals are superimposed. The stereographic projection given in Fig. 7c demonstrates that these alpha orientations had approximately equivalent relations with a single beta orientation.

No internal twinning was observed within the martensite units of the beta quenched alloy even though it has generally been seen that the plate morphology is associated with an internally twinned substructure [10]. However, as several workers have pointed out [11–13], this association between morphology and substructure may be purely coincidental. The dislocation structure resulting from the lattice invariant shear as well as from the accommodation stresses was found to be very irregular and it was not possible to identify the lattice invariant shear system. Typical dislocation structures are shown in Fig. 8. The beta quenched alloy also showed extensive precipitation – predominantly along the dislocations present in the structure (Fig. 9). The combination of the complex dislocation structure and the fine precipitate distribution made it difficult to characterize the martensite substructure.

Keys *et al.* [6] have found that the martensite in a Zr–1.8 wt% Cr alloy is an internally twinned plate martensite. In fact, these authors have observed that even in a Zr–1.0 wt% Cr alloy, a fraction of the martensite crystals are internally twinned. Warren and Ytterhus [14] have observed the presence of internally twinned martensite plates in a Zr–2 at % Cr–0.16 at.% Fe alloy. The absence of twinning in the martensite plates in the alloy used in the present work appeared to be inconsistent with these earlier observations. Banerjee and Krishnan [10] have suggested that in zirconium alloys, twinning occurs in the martensite crystals when the M_s temperature is lower than about 650° C. The M_s temperature of an alloy would be determined by the amount and the

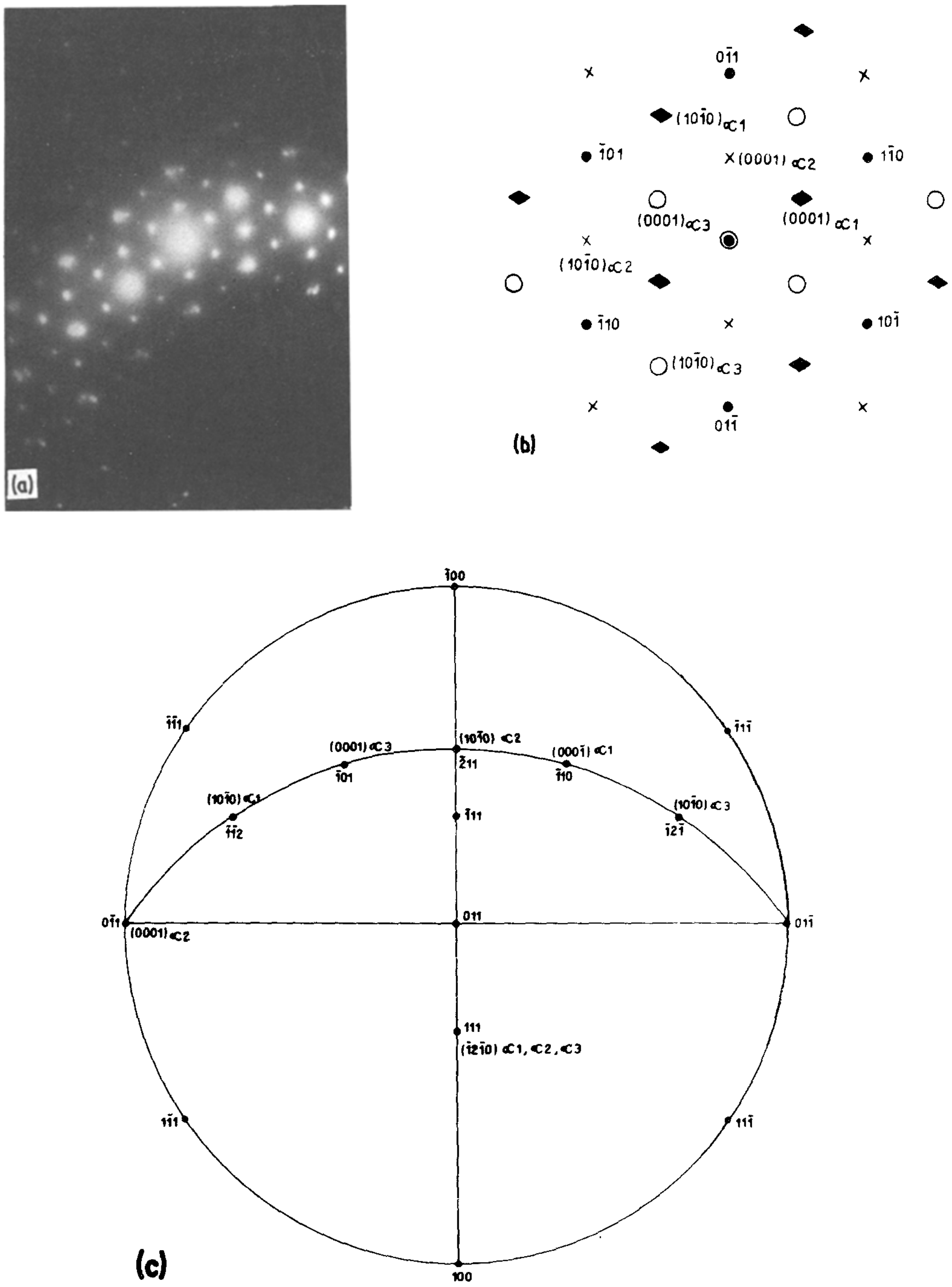

Figure 7 (a) Selected-area diffraction pattern showing the superposition of the reciprocal lattice sections corresponding to three different martensite crystals. (b) An idealized key to the diffraction pattern in (a) which shows the superposition of three alpha reciprocal lattice sections (all corresponding to the $\langle\bar{1}\,2\,\bar{1}\,0\rangle$ zone) on a $(1\,1\,1)_\beta$ section. (c) Stereogram illustrating the following relations between these alpha orientations (represented by α_1, α_2 and α_3) to a single beta orientation: $(0\,0\,0\,1) \parallel (1\,\bar{1}\,0)$ and $[\bar{1}\,2\,\bar{1}\,0] \parallel [1\,1\,1]$ for α_1; $(0\,0\,0\,1) \parallel (0\,\bar{1}\,1)$ and $[\bar{1}\,2\,\bar{1}\,0] \parallel [1\,1\,1]$ for α_2; $(0\,0\,0\,1) \parallel (\bar{1}\,0\,1)$ and $[\bar{1}\,2\,\bar{1}\,0] \parallel [1\,1\,1]$ for α_3.

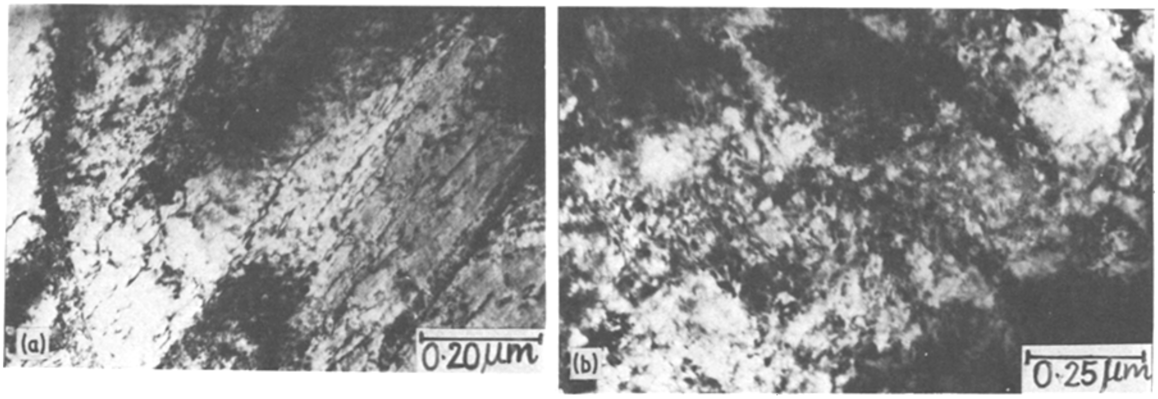

Figure 8 Typical dislocation substructures observed in the martensitic crystals in the beta quenched alloy.

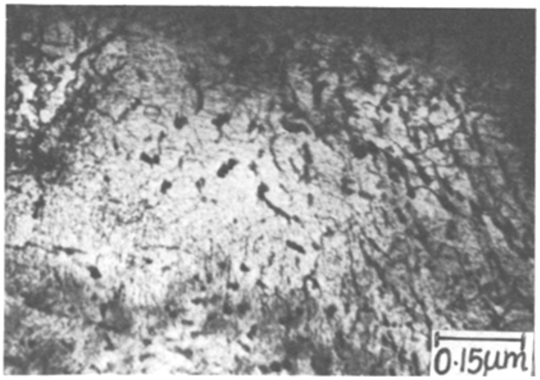

Figure 9 Precipitation in the beta quenched alloy; there is a tendency for the precipitates to form along dislocations.

nature of the beta and the alpha stabilizers present in it. It was likely that the absence of internal twinning in the alloy used here was due to the fairly high level of alpha stabilizing interstitials (950 ppm oxygen and 60 ppm nitrogen) in it. Oxygen, a strong alpha stabilizer, could have counteracted the effect of chromium on the M_s temperature with the result that its value was much higher than what it would be in an oxygen-free alloy and not low enough to promote internal twinning. Keys *et al.* [6] have not reported the oxygen content of the alloy used by them; presumably it was quite low. The alloy used by Warren and Ytterhus contained only 150 ppm oxygen.

3.2. Effect of tempering

It was noticed that the morphological features of the martensite structure remained substantially unaltered on tempering at temperatures as high as 550° C (Fig. 10). Even on ageing at 700° C for 24 h, the optical microstructure of the alloy appeared to be quite similar to that observed in the beta quenched condition (Fig. 11). One point of difference, however, was the presence of a thin layer of a light etching phase at the prior beta grain boundaries in the tempered alloy. It was possible that in the beta quenched alloy the grain-boundary region contained a very small amount of non-martensitic alpha (unresolvable in the optical microscope) which grew to form a continuous film during the ageing process. Transmission electron microscopy of samples tempered at 700° C showed that recovery and recrystallization of the martensite structure had proceeded to a significant extent, resulting in the formation of a structure containing fine subgrains and grains of alpha and a distribution of coarse $ZrCr_2$ precipitates along the boundaries separating these crystals (Fig. 12). The interiors of these subgrains and grains were almost dislocation free. The regular dislocation arrangements, characteristic of tilt and twist boundaries, at the crystal interfaces suggested that this structure resulted from a recovery process. The presence of fully recrystallized grains along with the recovered structure implied that partial recrystallization had also occurred. However, equi-axed grains characteristic of a recrystallized structure were not formed at many regions, presumably due to the restrictions imposed on grain-boundary migration by the second phase dispersion formed during beta quenching and during the early stages of tempering. The final shapes assumed by the grains and the sub-grains were determined by this precipitate distribution. Some of these features are illustrated in Fig. 13. The dislocations of which the small-angle boundaries separating the recovered sub-grains were composed could be imaged with $\{0002\}$ reflections (Fig. 14) and, therefore, had a non-basal Burgers vector. It was possible that these dislocations had originated from the transformation

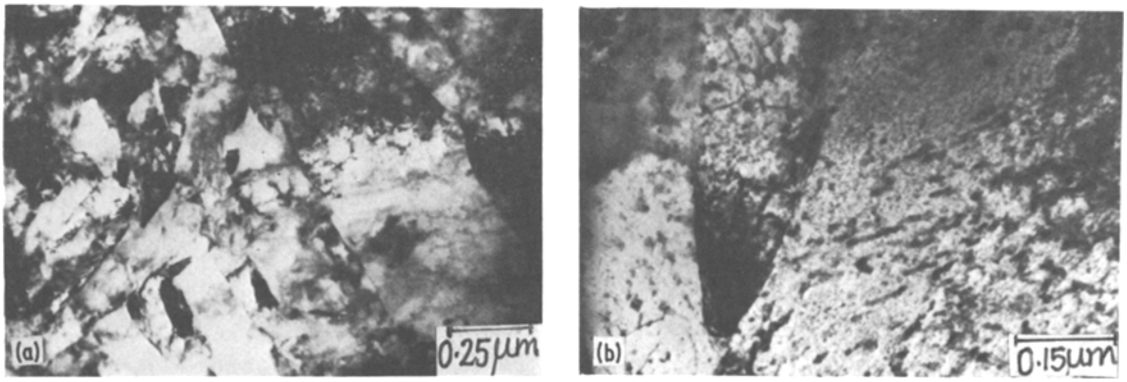

Figure 10 The retention of the martensite structure on ageing the beta quenched alloy at 550° C for 4 h.

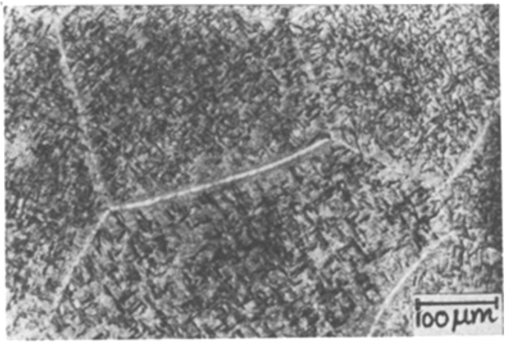

Figure 11 Typical microstructure, observed in a light microscope, of the alloy on ageing at 700° C for 24 h after beta quenching.

process and had subsequently rearranged themselves into regular arrays during tempering.

3.3. Omega precipitation

The presence of the omega phase could not be conclusively detected, either in the beta quenched or in the aged alloys, by X-ray diffraction. Still it was not possible to totally rule out the possibility of the formation of a small volume fraction of this phase during quenching in view of the observation that some "untransformed" grains were encountered in the light microscope. While doing transmission electron microscopy, in spite of scanning a large number of samples, it was not possible to hit upon a region which contained such "untransformed" grains. Earlier workers [6] have reported that these grains are actually constituted of a large number of fine omega crystals and that no prior beta phase is retained in these. In the present work, however, low microhardness values in the grain interiors precluded the possibility that these grains were composed entirely of omega crystals. The narrow band of the grain-boundary phase, referred to earlier in this paper, probably occurred due to the occurrence of a discontinuous reaction being either a direct eutectoid transformation ($\beta \rightarrow \alpha + ZrCr_2$) or a Widmanstatten precipitation of the alpha phase ($\beta \rightarrow \beta + \alpha$).

It has been suggested that the omega phase forms, on beta quenching, in those alloys of titanium [15] and zirconium [16] for which the electron-to-atom ratio lies between 4.14 and 4.15.

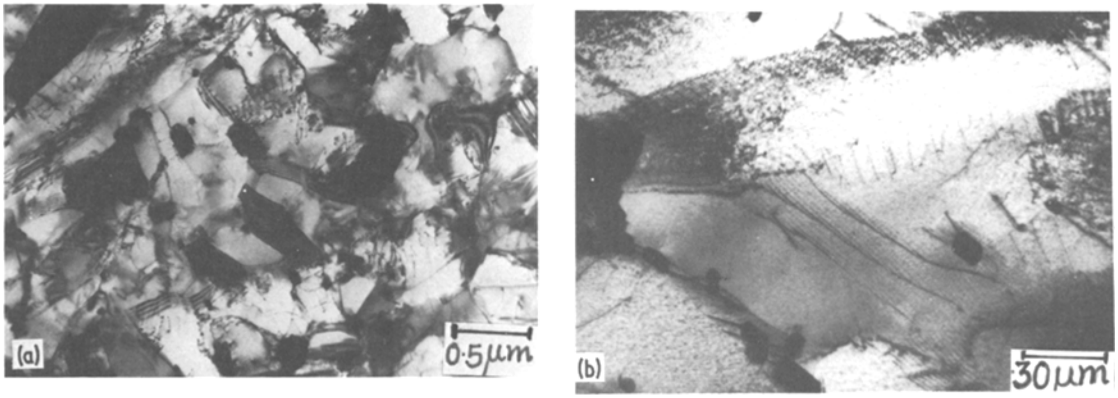

Figure 12 Typical structure of the alloy on ageing at 700° C. Coarse $ZrCr_2$ precipitates could be noticed at the grain and the subgrain boundaries.

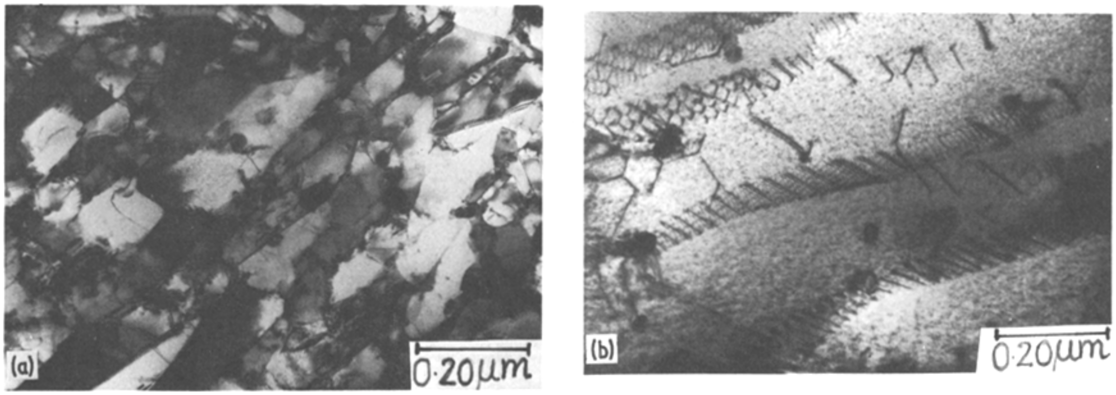

Figure 13 Elongated recrystallized grains, and (b) regular dislocation arrays observed on ageing the beta quenched alloy at 700° C.

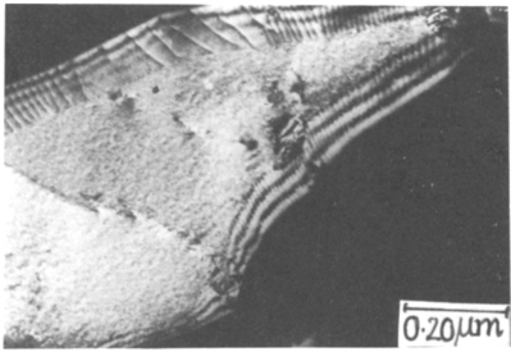

Figure 14 Zr–1.9 wt % Cr alloy, beta quenched and aged at 700° C for 4 h. Dark-field image of dislocations constituting a small-angle boundary (defining a recovered subgrain) under the (0 0 0 2) reflection.

According to Luke *et al.* [17], omega formation occurs over a range of electron concentration: 4.06 to 4.14. In the alloy used here, this ratio was about 4.06 – just on the threshold of the range promoting omega formation. However, Cometto *et al.* [18], Hickman [19] and Vanderpuye and Midownik [20] have shown that the empirical correlations between the electron to atom ratio and the occurrence of this phase are not strictly valid. Again, in view of the high level of alpha stabilizing interstitial elements present in this alloy, the amount of chromium contained in it might not have been sufficient for bringing about beta retention and/or omega precipitation. Even if the omega phase did form, its volume fraction must have been very small.

4. Conclusions

The martensite produced on quenching a Zr–1.9 wt % Cr alloy rapidly from the beta field has, in general, a plate morphology and a dislocated substructure. Neighbouring martensite crystals are often twin related, the twin plane being of the $\{1 0 \bar{1} 1\}_\alpha$ type. The martensite structure is quite stable at 550° C. However, tempering at 700° C causes recovery and recrystallization to occur, the shapes of the recrystallized grains being determined by the distribution of heterogeneously nucleated $ZrCr_2$ precipitates formed during beta quenching and during the early stages of tempering.

Acknowledgements

The authors are thankful to Dr V. M. Padmanabhan and Dr M. K. Asundi for their interest in this work and for helpful discussions. The assistance of Miss J. Agarwal at several stages of this investigation is gratefully acknowledged.

References

1. R. F. DOMAGALA, D. J. McPHERSON and M. HANSEN, *Trans. AIME* 197 (1953) 279.
2. W. ROSTOKER, *J. Metals* 5 (1953) 304.
3. W. M. RUMBALL and F. G. ELDER, *J. Less Common Metals* 19 (1969) 345.
4. E. T. HAYES, A. H. ROBERTSON and M. H. DAVIES, *Trans. AIME* 194 (1952) 304.
5. B. S. HICKMAN, *J. Mater. Sci.* 4 (1969) 554.
6. L. H. KEYS, G. JOHANSON and A. S. MALIN, *J. Nucl. Mater.* 59 (1976) 137.
7. S. BANERJEE and R. KRISHNAN, *Acta Met.* 19 (1971) 1317.
8. J. W. CHRISTIAN, "The Theory of Transformations in Metals and Alloys" (Pergamon Press, Oxford, 1965) p. 883.
9. W. G. BURGERS, *Physica* 1 (1934) 561.
10. S. BANERJEE and R. KRISHNAN, *Met. Trans.* 4 (1973) 1811.
11. J. W. CHRISTIAN, Special Report No. 93, "Physical Properties of Martensite and Bainite" (The Iron and Steel Institute, London, 1965).
12. S. BANERJEE, S. J. VIJAYAKAR and R. KRISHNAN, "Titanium Science and Technology", Vol. 3 (Plenum Press, New York, 1973) p. 1597.

13. S. BANERJEE, Ph.D. Thesis, Indian Institute of Technology, Kharagpur (1973).
14. M. R. WARREN and J. A. YTTERHUS, *Canad. Met. Q.* **11** (1972) 249.
15. Yu. A. BAGARYATSKIY, G. I. NOSOVA and T. V. TAGUNOVA, *Sov. Phys. Dokl.* 3 (1959) 1014.
16. Y. F. BYCHKOV, *Inzhener Fig. Zbur. Adak. Nauk. Belorus SSSR* 3 (1960) 95.
17. C. A. LUKE, R. TAGGART and D. H. POLONIS, *Trans. ASM* 57 (1964) 143.
18. P. J. COMETTO, G. L. HOUZE and R. F. HEHEMANN, *Trans. Met. Soc. AIME* **242** (1968) 2461.
19. B. S. HICKMAN, *ibid* **245** (1969) 1329.
20. N. A. VANDERPUYE and A. P. MIDOWNIK, "The Science, Technology and Application of Titanium" (Pergamon Press, Oxford, 1970) p. 719.

Received 9 August and accepted 2 October 1978.